PCCP

ROYAL SOCIETY OF CHEMISTRY

PAPER

View Article Online
View Journal | View Issue

Cite this: *Phys. Chem. Chem. Phys.*, 2024, **26**, 16008

Partitioning photochemically formed CO_2 into clathrate hydrate under interstellar conditions†

Gaurav Vishwakarma,[a] Bijesh K. Malla,[a] Rajnish Kumar *[bc] and Thalappil Pradeep *[ac]

Received 6th April 2024,
Accepted 16th May 2024

DOI: 10.1039/d4cp01414f

rsc.li/pccp

Clathrate hydrates (CHs), host–guest compounds of water forming hydrogen-bonded cages around guest molecules, are now known to exist under interstellar conditions. Experimental evidence demonstrated that prolonged thermal treatment of a solid mixture of water and CO_2/CH_4 produces CHs at 10–30 K under simulated interstellar conditions. However, in the current study, we show that CO_2 produced photochemically by vacuum ultraviolet irradiation of H_2O–CO mixtures at 10 K and $\sim 10^{-10}$ mbar, gets partitioned into its CH phase and a matrix phase embedded in amorphous ice. The process occurring under simulated interstellar conditions was studied at different temperatures and H_2O–CO compositions. The formation of CO_2 CH and other photoproducts was confirmed using reflection absorption infrared spectroscopy. The UV-induced photodesorption event of CO_2 may provide the mobility required for the formation of CHs, while photoproducts like methanol can stabilize such CH structures. Our study suggests that new species originating during such energetic processing in ice matrices may form CH, potentially altering the chemical composition of astrophysical environments.

Introduction

Energetic processes, like photoirradiation, are key in shaping the composition of cometary and interstellar ices. Such processes significantly influence the chemical and physical properties of these ices by generating radicals and reactive species.[1] These products can undergo recombination, diffusion, and reactions, potentially forming secondary products and getting trapped within the ice.[1–3] However, the trapping of photoproducts in clathrate cages during vacuum ultraviolet (VUV) irradiation of interstellar ice analogues has not been observed yet.

Clathrate hydrates (CHs) are inclusion compounds where water hosts and encases guest molecules like CH_4, CO, CO_2, and H_2S within its H-bonded cages.[4] CHs exist naturally in two structures, sI, and sII, in permafrost and marine sediments under high pressures and low temperatures.[4,5] However, CHs in interstellar-like environments have also been established experimentally,[6–15] and they have stimulated some scientific debate.[16,17] In one of our previous studies,[7] we had seen that when an ice mixture containing water and CH_4/CO_2 was subjected to extended annealing at 10–30 K in an ultrahigh vacuum (UHV), CH was formed. This study led to the speculation that photochemically produced molecules might also form CH. Shi *et al.*[18] observed that UV photons caused the trapping of O_2 (in turn, O_3 and H_2O_2) in porous water ice. They demonstrated that irradiation-induced trapping of O_2 in porous water ice is about seven times larger than equilibrium adsorption in the absence of irradiation. Bahr *et al.*[19] also reported the trapping of O_2 and H_2O_2 during the radiolysis of water ice between 40–120 K. Similarly, Fleyfel and Devlin reported the formation of CO_2 CH in a study where they subjected a simple ethylene oxide CH film to electron beam (1.7-MeV) irradiation at 15 K, and heated the resulting ice mixture to 100 K.[20] These observations suggest the possibility of the existence of photochemically produced molecules as CH under UHV and cryogenic conditions. However, there have been no studies in this regard.

Recombination, stabilization, and preservation of reactive molecules and free radicals in solid structures require cryogenic temperatures. Consequently, there has been widespread interest in developing methods to stabilize these reactive substances at higher temperatures.[21] The trapping of such species within CH cages offers a potential solution to this challenge. CH cages may hold such species up to their decomposition temperatures or till the sublimation of ice matrices. Capturing such species, even as they are generated during energetic

[a] *DST Unit of Nanoscience (DST UNS) and Thematic Unit of Excellence (TUE), Department of Chemistry, Indian Institute of Technology Madras, Chennai 600036, India. E-mail: pradeep@iitm.ac.in*
[b] *Department of Chemical Engineering, Indian Institute of Technology Madras, Chennai 600036, India. E-mail: rajnish@iitm.ac.in*
[c] *International Centre for Clean Water, IIT Madras Research Park, Chennai 600113, India*

† Electronic supplementary information (ESI) available: List of photochemical products, temperature and irradiation time-dependent RAIR spectra of pure CO and H_2O–CO films, SIMS spectrum of the irradiated H_2O–CO mixture. See DOI: https://doi.org/10.1039/d4cp01414f

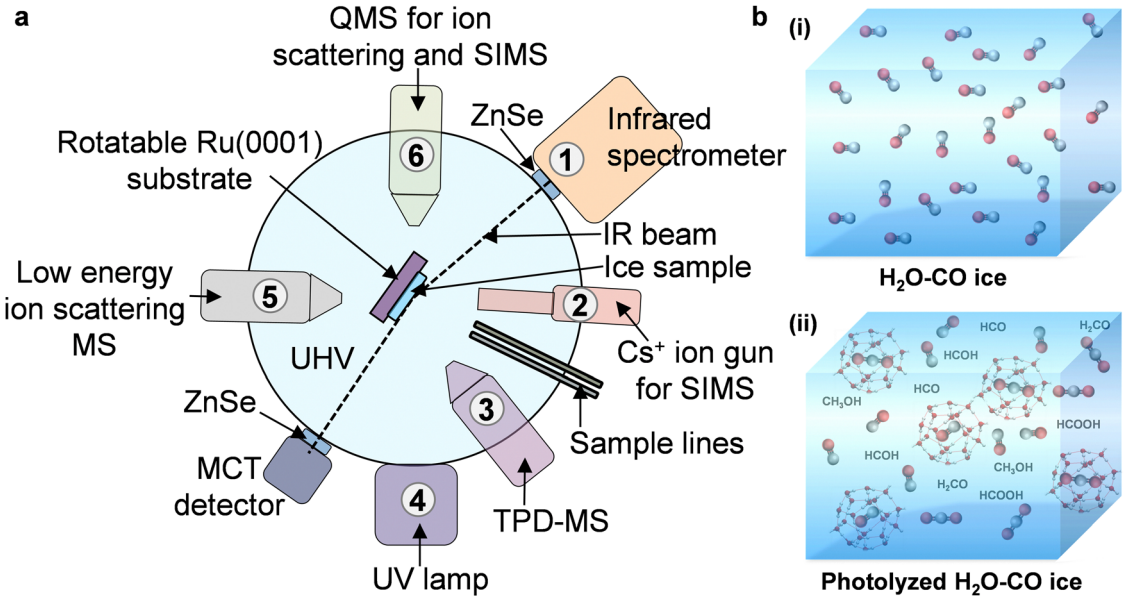

Fig. 1 (a) Schematic of the UHV apparatus. Various tools attached to the UHV chamber are (1) RAIRS setup with ZnSe window and MCT detector, (2) Cs^+ ion gun, (3) TPD-MS setup, (4) UV lamp, (5) low energy ion scattering setup, and (6) quadrupole mass analyzer. The substrate, in the schematic, is oriented for RAIR measurements. (b) Schematic illustration of the composition of H_2O–CO mixture (i) before and (ii) after VUV irradiation at 10 K, where the blue cube represents the water matrix.

processes like photon irradiation, holds high significance in planetary science, astrochemistry, and physical chemistry. In cold, dense molecular clouds, H_2O and CO dominate the grain mantles.[22,23] By mimicking such environments, extensive laboratory studies have been conducted exposing the H_2O–CO system to various stimuli (photon, electron, and ion irradiation) to comprehend the formation and evolution of several interstellar molecules. However, the trapping of secondary products during VUV irradiation of H_2O–CO ice remains unexplored. The present study investigates the physicochemical fate of photochemically produced CO_2 from an H_2O–CO mixture co-deposited at 10 K. The process has been studied at different temperatures and H_2O–CO compositions. The evolution of the H_2O–CO mixture upon VUV exposure under UHV and cryogenic conditions was monitored by reflection absorption infrared spectroscopy (RAIRS), and temperature-programmed desorption (TPD) mass spectrometry using a custom-built UHV setup, illustrated in Fig. 1a and described in detail elsewhere.[24]

Experimental methods

Experimental setup

The experimental setup was the same as the one we used to prepare clathrate hydrate (CH) at a cryogenic temperature under ultrahigh vacuum (UHV),[7,8] and was described in detail elsewhere.[24] Briefly, the apparatus consisted of a UHV chamber (with a base pressure $\sim 5 \times 10^{-10}$ mbar), a closed-cycle He cryostat, a gas inlet system, equipped with reflection absorption infrared spectroscopy (RAIRS), temperature-programmed desorption (TPD) mass spectrometry, Cs^+ ion-based secondary ion mass spectrometry (SIMS), low energy ion scattering (LEIS) mass spectrometry, and an ultraviolet (UV) lamp. The thin ice films were created on cold Ru(0001) substrate. The substrate is mounted at the cold end of the He cryostat and fitted with a precision x–y–z–θ sample manipulator that can be reoriented to do various measurements, as shown in Fig. 1a. The substrate temperature could be adjusted using a resistive heater (25 Ω) in the 8–1000 K range and measured by different thermal sensors (K-type thermocouple and a platinum sensor) with a temperature accuracy/uncertainty of 0.5 K. The substrate temperature was controlled by a temperature controller (Lakeshore, Model 336).

Materials and reagents

CO (99.5%) gas was purchased from Rana Industrial Gases & Products and was used without further purification. Millipore water (H_2O of 18.2 M Ω resistivity) was taken in a vacuum-sealed test tube and further purified *via* several freeze–pump–thaw cycles.

Sample preparation

Thin ice films were prepared by vapor deposition on the pre-cooled Ru(0001) substrate at 10 K. The molecular vapor deposition was controlled by two high-precision all-metal leak valves through two inlet lines that were directed to the middle of the substrate. Out of two inlet lines, one was exclusively used for CO and the other for H_2O. The molecular deposition coverage was expressed in monolayers (ML) assuming 1.33×10^{-6} mbar $s = 1$ ML, estimated to contain $\sim 1.1 \times 10^{15}$ molecules cm^{-2}, as adopted in earlier studies.[7,8] The purity and ratio of the CO and H_2O ice mixtures were further confirmed during vapor deposition using a residual gas analyzer. Also, the Ru(0001) substrate was repeatedly heated to 400 K prior to each vapor deposition

in order to ensure that the surface was sufficiently clean for the current study. Prior to the current set of experiments, the substrate was polished and annealed at 1000 K.

Determination of the column density (N) and UV lamp flux

We applied the extensively used method[25] to estimate the column density of absorbing molecules.

$$N_M = S_M/A_M$$

Where N_M is the column density of molecule M in cm^{-2}, S_M is the integrated area of the specific IR band of molecule M, and A_M is the band strength of the same band in cm $molecule^{-1}$. The values of H_2O column densities in mixed H_2O–CO film were estimated as $N_{H_2O} = S_{H_2O}/A_{H_2O}$, where S_{H_2O} was the integrated area of the 1670 cm^{-1} band, A_{H_2O} (8×10^{-18})[25] was the strength of the band absorption. Similarly, the values of CO column densities were estimated as $N_{CO} = S_{CO}/A_{CO}$, where S_{CO} was the integrated area of the 2180–2110 cm^{-1} band, A_{CO} (2×10^{-17})[25] was the strength of the band absorption. In the present work, the ratios of the H_2O–CO mixture were estimated by dividing the column densities of H_2O with CO for each ice sample.

A deuterium lamp (McPherson, Model 634, with MgF_2 window, 30 W) of vacuum ultraviolet (VUV) range, 115–300 nm, was used as the UV light source. The VUV lamp was differentially pumped and attached to the UHV chamber through the MgF_2 window (with a cut-off at ~114 nm (10.87 eV)). The UV lamp flux was determined by applying the widely used ozone method ($O_2 \rightarrow O_3$ conversion)[26,27] where solid O_2 was VUV photolyzed at 10 K. The average photon flux reaching the ice sample was estimated to be $\sim 6 \times 10^{12}$ photons cm^{-2} s^{-1}.

Experimental protocol

For VUV photoprocessing, the H_2O–CO mixture was prepared by co-depositing H_2O and CO vapors on Ru(0001) at 10 K. The sample preparation method is the same as adopted in our previous studies.[7,8,13] Briefly, ice films of ~100 ML of H_2O and CO were prepared by backfilling the vacuum chamber at a total pressure of $\sim 5 \times 10^{-7}$ mbar for 3 min 20 s, starting from a base vacuum of $\sim 5 \times 10^{-10}$ mbar. For the co-deposition of H_2O and CO in a 1 : 1 ratio, the inlet pressure of H_2O was kept $\sim 2.5 \times 10^{-7}$ mbar and that of CO was $\sim 2.5 \times 10^{-7}$ mbar. Here, the deposition coverages were measured as the product of the dosing time and the chamber pressure of exposure. However, here, the ratio of H_2O to CO in the resulting H_2O–CO mixture was estimated by dividing the column densities of H_2O with CO. Each experiment was carried out in two steps. In the first step, after several heating–cooling cycles, a background RAIR spectrum of the clean substrate was recorded. Then mixed ice composed of H_2O and CO (of desired ratios) was prepared on the Ru(0001) at 10 K. After sample preparation at 10 K, a RAIR spectrum of the unirradiated ice sample was recorded. Then, the substrate was reoriented to expose the as-prepared sample to VUV irradiation. In the second step, the UV lamp was switched on, exposing the sample to VUV radiation for a desired period. After each irradiation, the substrate was again reoriented to RAIRS configuration to record the IR spectra of the irradiated ice film.

VUV photolysis experiments were performed in two sets, (1) temperature-dependent and (2) H_2O–CO composition-dependent photolysis. In the first set, an H_2O–CO mixture of a fixed composition (H_2O to CO ratio 7.93 ± 0.19) was prepared at 10 K and was isothermally irradiated at the corresponding temperatures of 10, 20, and 30 K. For 20 and 30 K experiments, the ice samples were prepared at 10 K and annealed to the set temperatures at an annealing rate of 2 K min^{-1}. In the second set, mixed ice of three different ratios of H_2O–CO (with H_2O to CO ratio = 1.46, 4.09, and 7.72) was prepared and irradiated at 10 K. For both sets of experiments, the ice sample was irradiated for four hours, and RAIR spectra were collected, at 0, 0.5, 1, 1.5, 2, 3, and 4 h.

RAIRS setup

Before and after VUV irradiation of ice samples, RAIR spectra were collected using a Bruker Vertex 70 FT-IR spectrometer in the 4000–550 cm^{-1} range with a spectral resolution of 2 cm^{-1}. For a better signal-to-noise ratio, each RAIR spectrum was averaged over 512 scans. During experiments, the IR beam was focused on the ice sample at an incident angle of 80° ± 7° through an infrared transparent ZnSe viewport. The reflected beam from the ice sample was recorded with a liquid nitrogen cooled mercury cadmium telluride (MCT) detector. The IR beam outside the vacuum chamber was purged with dry nitrogen to avoid background noise.

TPD-MS setup

For the TPD-MS experiment, H_2O–CO (1.46) mixture was prepared at 10 K, and the resulting ice sample was exposed to VUV irradiation for 2 h. After irradiation, TPD experiments were performed by rotating the substrate in the TPD configuration. Each TPD experiment was performed at a 30 K min^{-1} heating rate. The thermal desorption profile of CO, CO_2, and H_2O was recorded by monitoring the m/z = 28, 44, and 18, respectively, as a function of substrate temperature.

The TPD module (Extrel CMS) was attached to the vacuum chamber on a 6-inch flange through a Z-axis manipulator. The module consisted of an electron impact source, a mass analyzer, and a detector. The mass analyzer was a quadrupole with 1 to 500 mass range and 1 amu resolution.

SIMS setup

We have conducted ion collision experiments on the H_2O–CO ice surface using Cs^+ of 60 eV kinetic energy produced from a low-energy alkali ion gun (Kimball Physics Inc.). Cs^+ (m/z 133) is a well-known projectile for SIMS. This technique is sensitive only to the first few layers of the surface. The low energy collision of Cs^+ converts the neutral adsorbate species (M) to gas phase ions (CsM^+) by association reaction in a process widely known as reactive ion scattering (RIS). The resulting scattered ions were analyzed using a quadrupole mass analyser. We have used the RIS signal intensities corresponding to the complex of Cs^+ with H_2O {m/z = 151 ($Cs(H_2O)^+$), m/z = 169

$(Cs(H_2O)_2^+)$, m/z = 187 $(Cs(H_2O)_3^+)$, *etc.*}, with CO {m/z = 161 $(Cs(CO)^+)$, m/z = 189 $(Cs(CO)_2^+)$, m/z = 217 $(Cs(CO)_3^+)$, *etc.*}, and with CO–H_2O complexes {m/z = 179 $(Cs(CO–H_2O)^+)$, m/z = 197 $(Cs(CO–(H_2O)_2)^+)$, m/z = 207 $(Cs((CO)_2–H_2O)^+)$, *etc.*} to identify the surface structure of H_2O–CO mixture. Here, the signal intensities are directly proportional to the surface population of the molecule (or complex) on the ice surface.

Results and discussion

To begin with, H_2O–CO (1.46) mixture was exposed to VUV irradiation for 2 h at 10 K (details of experimental protocol are given in Experimental method). Full range RAIR spectra collected before and after irradiation are shown in Fig. S1 (ESI†). The photoproducts produced in the process are listed in Table S1 (ESI†). The photochemical products, CO_2, HCO, H_2CO, CH_3OH, and HCOOH, observed in the current work, are consistent with the earlier studies.[25,28] However, evidence of the formation of CH was observed and discussed for the first time in the current work. A schematic illustration of the composition of the ice mixture before (i) and after (ii) VUV exposure to the H_2O–CO mixture is shown in Fig. 1b. Moreover, in a VUV experiment conducted on pure CO ice, we could not observe any photoproducts with RAIRS (intensity of the CO absorption band does not decrease), as shown in Fig. S2 (ESI†). Literature supports this observation.[29,30] However, Gerakines *et al.*[31] observed the formation of CO_2 and other photoproducts through the involvement of excited species, as CO + $h\nu$ → CO*; CO* + CO → CO_2 + C.

Fig. 2 shows the RAIR spectra for 0 h (black trace) and 2 h (blue trace) VUV irradiation of H_2O–CO (7.72) mixture at 10 K in the C=O antisymmetric stretching region of CO_2 (a) and C = O stretching region of CO (b). In Fig. 2a, at 0 h (without irradiation), the flat line suggests the absence of CO_2 in the H_2O–CO mixture. However, after 2 h of VUV irradiation, two peaks at 2353 and 2346 cm^{-1} were observed, which are attributed to CO_2 that exists in amorphous solid water (ASW) pores and CH cages (512 cage of sI),[4,32] respectively. The assignments are consistent with the previous studies.[7,14,33,34] Notably, in our present study, we did not detect the IR peak corresponding to CO_2 confined within the large cage ($5^{12}62$) of sI, which would typically occur around ~2337 cm^{-1}.[33] It is worth noting that a similar observation has been reported by both Blake *et al.*[14] and Ghosh *et al.*[7] The CO_2 partitioning in ASW *versus* CH cages has been studied extensively.[14,15,35] However, significant differences exist between the experimental conditions of the current work and those of the literature. While, the current study observes CO_2 CH formation under UHV at 10 K through VUV irradiation. Previous studies by Blake *et al.* and Netsu *et al.* noted the formation of CO_2 CH at ~120 K under high vacuum (HV), with and without CH_3OH, respectively. Similarly, Bauer *et al.* observed its formation at 194 K under HV while warming a CO_2–H_2O amorphous mixture. It should be noted that the vacuum conditions influence both the sublimation temperature and mobility of water and other molecules, which are critical for CH formation.

To further confirm our RAIRS assignments, we heated the photolyzed H_2O–CO ice beyond the desorption temperature of CO_2, around 90 K in a control experiment (Fig. S3, ESI†). The peak at 2353 cm^{-1} disappeared suggesting the desorption of free CO_2 from water matrix, while the peak at 2346 cm^{-1} persisted manifesting the trapping of CO_2 in the clathrate cages.[7] This confirmed that the photochemically produced CO_2 at 10 K is partitioned into the ASW matrix and the CH phase. In the current study, the formation of CH did not lead to a noticeable change in the O–H stretching band (Fig. S1, ESI†). This could be due to the following reasons. We observed in our earlier studies[9,10,13] that the spectral features of O–H remained broad[35] even after CH formation. This may be due to the fact

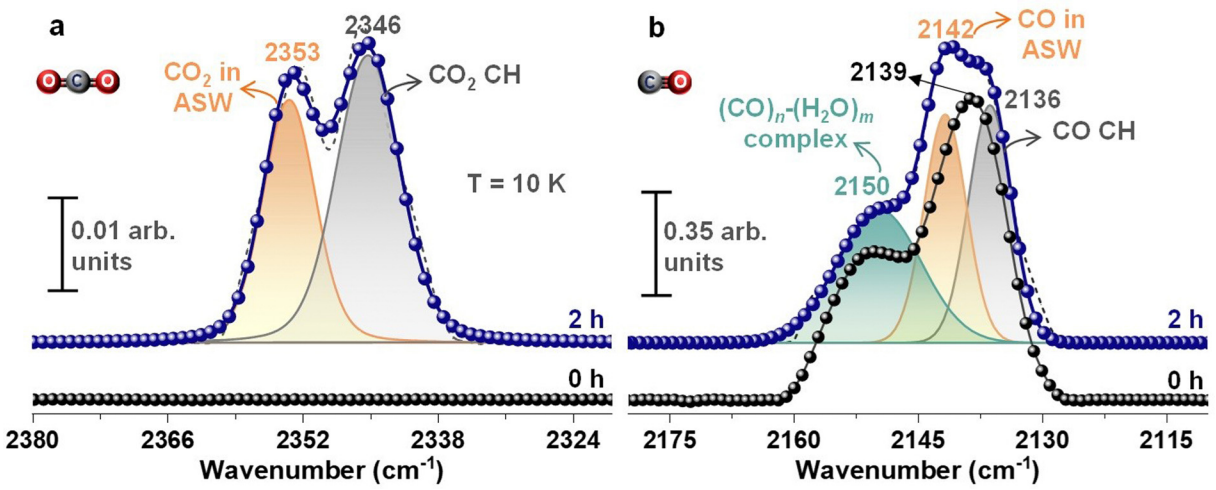

Fig. 2 RAIRS analysis of the formation of CO_2 and CO CH. RAIR spectra before (0 h, black curve) and after VUV irradiation (2 h, blue curve) of 100 ML H_2O–CO (7.72) mixture at 10 K in the (a) C=O antisymmetric stretching region of CO_2, and (b) C=O stretching region of CO. While the peak at 2346 cm^{-1} in (a) arises due to the formation of CH of CO_2, the peak at 2136 cm^{-1} in (b) is due to the formation of CH of CO at 10 K. The normalized RAIR spectrum (of 2 h) in (b) was deconvoluted to demonstrate the existence of different CO phases, namely, 2150 cm^{-1} (CO···H_2O complexes), 2142 cm^{-1} (pure CO), and 2136 cm^{-1} (CO CH). For clarity, the spectra in (b) are normalized to 1 in absorbance.

that the CH is distributed in small domains across the ASW matrix, rather than forming an extended crystalline phase under UHV conditions. It should also be noted that UV irradiation causes amorphization of the ordered structure.[36]

Moreover, in Fig. 2b at 0 h, there are two peaks at ~2150 and 2139 cm^{-1} in the C═O stretching region of CO, which are attributed to hydrogen-bonded complexes of CO and H_2O as well as CO in the ASW matrix, respectively.[37,38] Pure solid CO at 10 K shows an absorption peak at 2142 cm^{-1} (Fig. S2, ESI†). In Fig. 2b, after 2 h of VUV irradiation, three peaks were observed at 2150 (broad), 2142, and 2136 cm^{-1}, which are attributed to CO···H_2O complexes, pure CO ice, and CH of CO, respectively.[37–39] The assignment to 2136 cm^{-1} peak as due to CH of CO is supported by previous infrared analysis.[38,39] These studies suggested a redshift of ~5 cm^{-1} for the absorption peak of CO within the CH cage, compared to pure CO. Thus, the photolysis of H_2O–CO mixture at 10 K under UHV led to not only the creation of new chemical compounds but also the formation of CH of CO and CO_2 within the ice matrix.

Further, TPD experiments were performed to confirm the formation of CHs of CO and CO_2. It has been shown that the trapped molecules, inside the pores, in CH cages or buried inside the ASW matrix, desorb during amorphous-to-crystalline ice transition as well as during matrix sublimation.[7,35,40–42] In our previous studies performed under similar conditions,[7,11] we have seen an abrupt release of guest molecules, such as CO_2, CH_4, and C_2H_6 trapped in CH cages and from ice matrix during the amorphous-to-crystalline transition, in an event termed as a molecular volcano (MV).[43] Fig. 3a shows the desorption of CO (m/z = 28), CO_2 (m/z = 44), and H_2O (m/z = 18) from the photolyzed H_2O–CO (1.46) mixture obtained during 30 K min^{-1} TPD experiment. The peaks marked *, $, and # are attributed to the desorption of submonolayer CO, desorption of CO/CO_2 due to the structural transition in the ice matrix during annealing, and co-sublimation of CO/CO_2 along with water, respectively. The peaks at 25 and 38 K for CO (blue trace) correspond to the desorption of multilayer CO, and the desorption of CO that hydrogen bonded with H_2O (CO···H_2O complexes), respectively. The peaks at 77 K for CO_2 (green trace) and at 155 K for H_2O (black trace) correspond to the desorption of multilayer CO_2, and sublimation of H_2O matrix, respectively. The inset in Fig. 3a shows a desorption peak at 140 K for CO and CO_2. The peak at 140 K corresponds to MV. Thus, the presence of MV peak for CO and CO_2 in TPD traces suggest the existence of

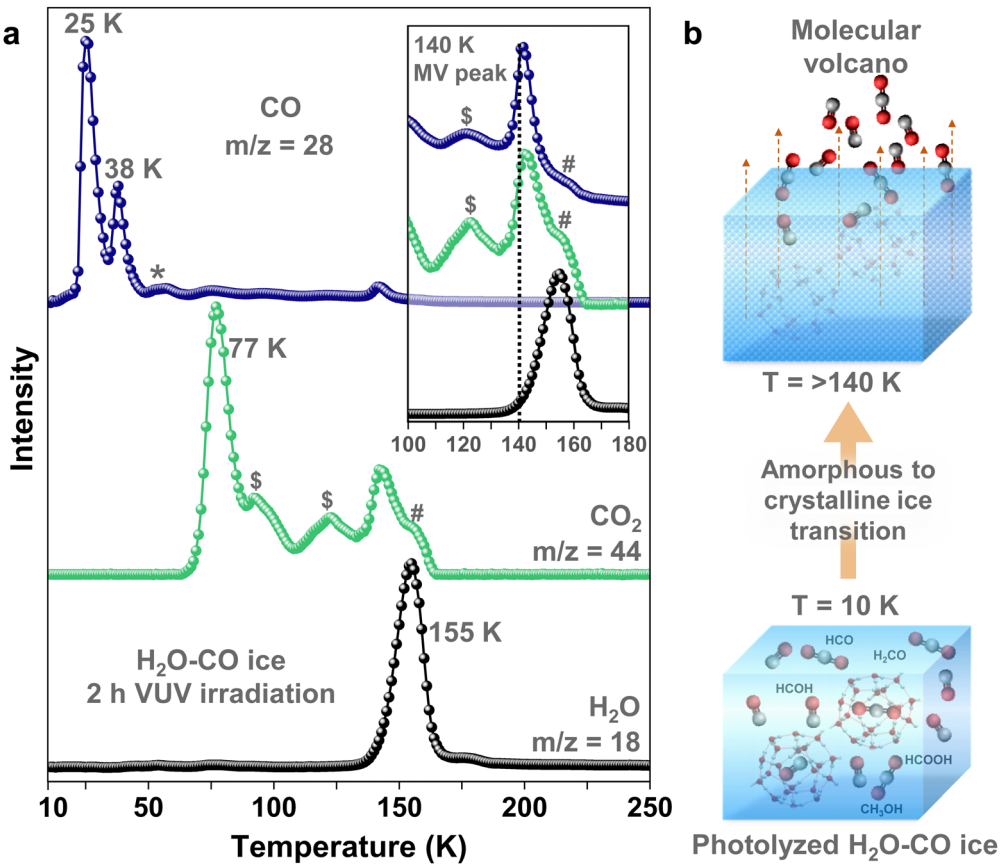

Fig. 3 TPD mass spectrometric analysis of photolyzed H_2O–CO mixture. (a) Desorption of CO, CO_2, and H_2O from photolyzed H_2O–CO mixture during 30 K min^{-1} TPD experiment. For this, 100 ML of H_2O–CO (1.46) mixture was co-deposited on Ru(0001) substrate at 10 K, and the resulting sample was exposed to VUV irradiation for 2 h. After irradiation, the substrate was annealed at a rate of 30 K min^{-1} to 250 K. The intensities of the m/z = 28 (CO), 44 (CO_2), and 18 (H_2O) were plotted as a function of substrate temperature. (b) Schematic illustration of the MV event during amorphous-to-crystalline ice transition above 140 K. To ensure clarity, only CO and CO_2 desorption events are shown.

their CHs in the ASW matrix.[7,11,35,40,41] Fig. 3b schematically represents the MV event during the amorphous-to-crystalline transition of H_2O above 140 K. In conclusion, RAIRS (Fig. 2) and TPD-MS (Fig. 3) studies of the photolyzed H_2O–CO mixture confirm the presence of CHs of CO and CO_2 in the ASW matrix.

Furthermore, the extent of photochemically produced CO_2 partitioning at different temperatures and H_2O–CO compositions was examined with RAIRS, and results derived from these experiments are presented in Fig. 4a and b. We examined the effect of temperature by subjecting an H_2O–CO mixture (with an approximately fixed composition, H_2O to CO ratio of 7.93 ± 0.19) to VUV irradiation for 4 h at 10, 20, and 30 K, and analyzed the resulting RAIR spectra. The spectral evolution of the dominant infrared peaks of CO (C═O stretching, 2180–2110 cm^{-1}) and CO_2 (C═O antisymmetric stretching, 2380–2320 cm^{-1}) are shown in Fig. S4a and b (ESI†). The integrated areas of these peaks are plotted as a function of irradiation time and the data are shown in Fig. S4c and d (ESI†). Fig. 4a is derived from Fig. S4d (ESI†) by normalizing the integrated band area of the 2380–2320 cm^{-1} region (representing total CO_2 produced) with respect to 2346 cm^{-1} (CO_2 in CH) and 2353 cm^{-1} (CO_2 in ASW). Here, the the area under the curve does not directly correlate with the column density for distinct phases of CO_2. The estimation of column density for the absorption bands at 2353 and 2346 cm^{-1} was not feasible due to the uncertainty surrounding their respective band strengths. Fig. 4a suggests that the fraction of CO_2 CH produced at 30 K after 0.5 h of VUV irradiation is larger than that produced at 10 and 20 K. The fraction of CO_2 CH produced at 10 and 20 K is almost equal. Notably, the initial fraction of CO in the H_2O–CO mixture was lower at 30 K, likely due to desorption of CO above 25 K (as shown in Fig. 3a). Further, we have extended our study to monitored the evolution of photochemically produced CH of CO_2 for longer VUV exposure of 4 h. We observed that, as the irradiation time increases (from 0.5 to 4 h), the fraction of CO_2 CH produced get reduced at all temperatures, as marked by the black arrow (Fig. 4a).

Similarly, we examined the effect of the H_2O–CO composition at 10 K using mixtures with different H_2O to CO ratios, 1.46, 4.09, and 7.72. The results derived from RAIRS study are presented in Fig. S5a–d (ESI†). Fig. 4b was derived from Fig. S5d (ESI†), as described above. The results in Fig. 4b indicate that after 0.5 h of irradiation, H_2O–CO mixtures with larger fractions of H_2O produce more CO_2 CH. Nevertheless, similar to Fig. 4a, with increasing irradiation time (from 0.5 to 4 h), the CO_2 trapped in CH decreased for all compositions as marked by the black arrow in Fig. 4b. In conclusion, the combined analysis of Fig. 4a and b revealed interesting trends. Higher temperatures and mixtures with larger H_2O fractions resulted in greater production of CO_2 CH after 0.5 h of photolysis. Moreover, in Fig. 4a and b, the overall decrease in the fraction of CO_2 CH (or increase in the fractions of CO_2 trapped in ASW) with irradiation time (from 0.5 to 4 h) can be attributed to the decomposition of CH structure, possibly by (i) exposure to VUV radiation,

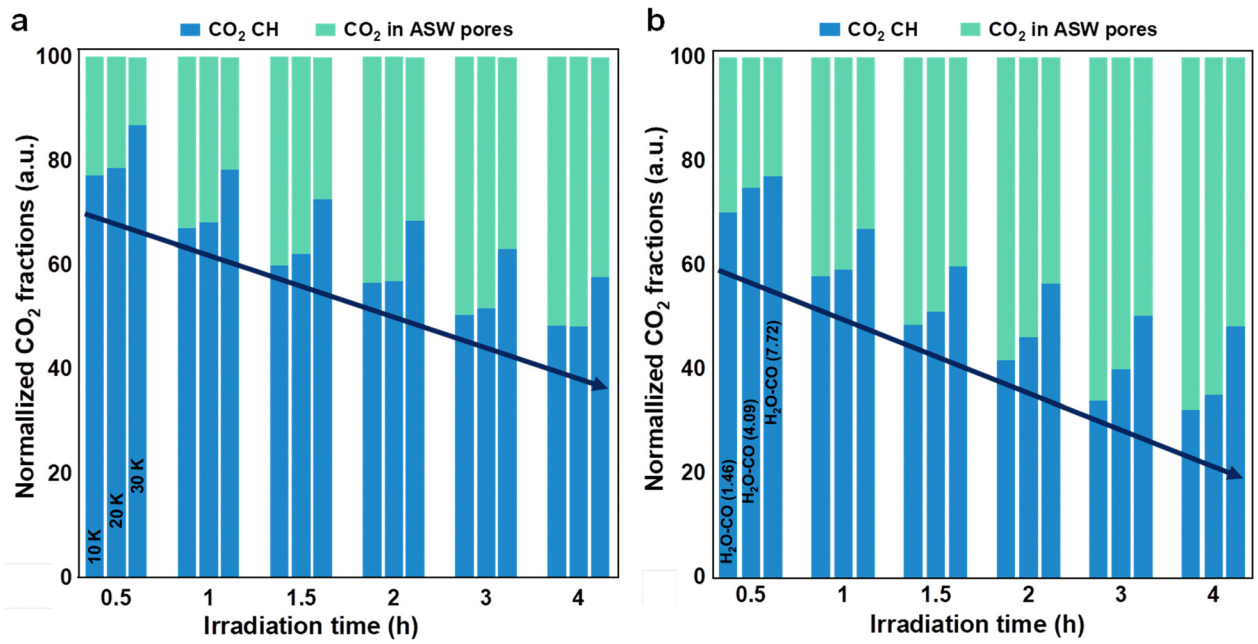

Fig. 4 Trends of photochemically produced CO_2 partitioning at different temperatures and H_2O–CO compositions. (a) Temperature-dependent partitioning of formed CO_2 with respect to VUV irradiation time. For each irradiation time, the first, second, and third columns represent the irradiation temperature, 10, 20, and 30 K, respectively. (b) Composition-dependent partitioning of the formed CO_2 with respect to VUV irradiation time. For each irradiation time, the first, second, and third columns represent the H_2O–CO composition of 1.46, 4.09, and 7.72, respectively. Here, shown is a stacked bar plot of the integrated band area of the photochemically partitioned CO_2 as the function of irradiation time. For this, band areas are derived from RAIRS data (Fig. S3b and S4b, ESI†) by deconvoluting the C═O antisymmetric stretching region of CO_2 (2380–2320 cm^{-1}). The fractions of the CO_2 CH phase, and CO_2 in ASW pores are shown by sky blue, and green, respectively. The decrease in the fraction of CO_2 CH with long VUV exposure time is marked by black arrows in (a) and (b). Fig. 4 has been modified as per the referee's suggestions.

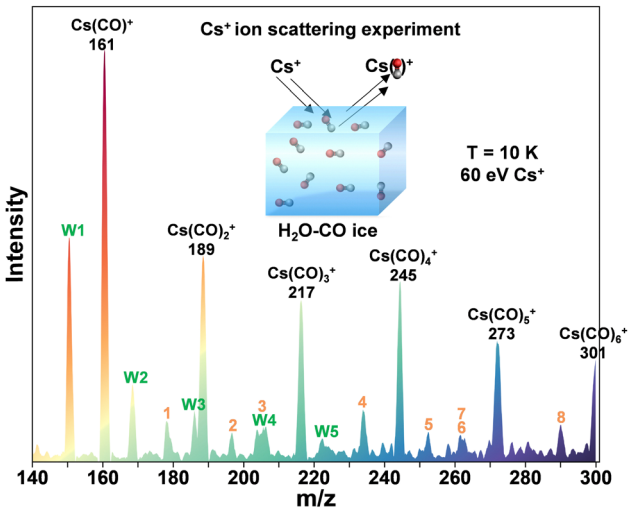

Fig. 5 Cs^+ ion scattering analysis of the surface of unirradiated H_2O–CO (1.46) mixture. The mass spectrum of the unirradiated H_2O–CO mixture was obtained by colliding the sample with 60 eV Cs^+ ions at 10 K. The peaks shown in the mass spectrum correspond to the adducts of Cs^+ (m/z = 133) with CO (m/z = 28), H_2O (m/z = 18), and CO···H_2O complexes. The adducts of $Cs(CO)_n^+$ are marked in the spectrum. The adducts of $Cs(H_2O)_n^+$ are marked by W1–W5, where W1 = $Cs(H_2O)_1^+$, and W5 = $Cs(H_2O)_5^+$. The adducts of Cs^+ with CO···H_2O complexes are marked as 1 (m/z = 179, (CO–H_2O)), 2 (m/z = 197, $CO(H_2O)_2$), 3 (m/z = 207, $H_2O(CO)$), 4 (m/z = 235, $H_2O(CO)_3$), 5 (m/z = 253, $(H_2O)_2(CO)_3$), 6 (m/z = 261, $(CO)_2(H_2O)_4$), 7 (m/z = 263, $H_2O(CO)_4$) and 8 (m/z = 291, $H_2O(CO)_5$). Inset illustrates a schematic representation of the Cs^+ ion scattering experiment.

and (ii) interactions of the photoproducts with H_2O of the CH structure. The CO_2 released after CH decomposition will migrate to the ASW matrix, increasing the CO_2 fraction in the ASW phase.[8]

During VUV irradiation, pure CO ice does not photodissociate (Fig. S2, ESI†). However, when mixed with H_2O, it resulted in several photochemical products[29,30] as presented in Fig. S1 (ESI†). We considered it important to investigate the structural characteristics of H_2O–CO ice at 10 K using highly surface-sensitive Cs^+-based secondary ion mass spectrometry.[44] The result obtained from the Cs^+ (m/z = 133) ion scattering experiment, by colliding the unirradiated H_2O–CO ice surface with 60 eV Cs^+ ions at 10 K, is shown in Fig. 5. The result shows that apart from the existence of intra-clusters of H_2O (W1–W5, where W1 = $Cs(H_2O)_1^+$, and W5 = $Cs(H_2O)_5^+$) and (CO ($Cs(CO)_1^+$, to $Cs(CO)_6^+$)) there exist a variety of inter-clusters of CO with H_2O as well, as marked by 1–8. For instance, 1 = $Cs(CO–H_2O)^+$, 2 = $Cs(CO(H_2O)_2)^+$, 3 = $Cs(H_2O(CO)_2)^+$, 4 = $Cs(H_2O(CO)_3)^+$, 5 = $Cs((H_2O)_2(CO)_3)^+$, 6 = $Cs((CO)_2(H_2O)_4)^+$, 7 = $Cs(H_2O(CO)_4)^+$ and 8 = $Cs(H_2O(CO)_5)^+$. The RAIR spectrum of the unirradiated H_2O–CO mixture presented in Fig. 2b shows a broad peak at ~2150 cm^{-1} in the C≡O stretching of CO. In previous infrared studies,[37,38,45,46] the peak was assigned to the existence of complex of CO and H_2O, $(CO)_n$–$(H_2O)_m$ as 1 : 1 complex. Several other experimental and theoretical simulations have studied the 1 : 1 CO···H_2O complex in detail.[46–48] However, complexes of $(CO)_n$–$(H_2O)_m$ with n, $m > 1$ have not been observed yet. In the current work, the complexes of $(CO)_n$–$(H_2O)_m$ with varying n and m have been detected for the first time, at the surface of H_2O–CO mixture at 10 K, owing to the high sensitivity of the ion pickup by Cs^+ ion scattering method. Ishibashi *et al.* revealed that the sensitivity of the Cs^+-based ion pickup approach in identifying extremely low abundant species on the ice surface is 100 times greater than that of FTIR, even for infrared-active molecules.[49] Thus, Fig. 5 presents a clear picture of the complexes formed on the surface of mixed H_2O–CO ice at 10 K. Furthermore, experimental and computational investigations are necessary to determine the precise structure and geometry of such $(CO)_n$–$(H_2O)_m$ complexes. Additionally, the photoproducts observed by RAIRS were further confirmed by performing Cs^+ ion scattering experiment on photolyzed H_2O–CO mixture as presented in Fig. S6 (ESI†).

While we have known the existence of CHs of stable molecules in the ISM,[6,7] the present study introduces a new possibility where the reaction products themselves can be incorporated into CH cages. Also, there is a great possibility of conversion of one guest molecule to another inside clathrate cages upon VUV irradiation. This could be a very exciting and unique experiment to be carried out in similar systems. Given that photochemistry can generate a wide range of species, this research presents the potential for various CH phases to exist in the ISM, albeit at potentially low concentrations. Furthermore, it suggests the possibility of enhanced thermodynamic stability for photochemical reaction products, which may serve as an additional factor facilitating the overall reaction. Although the diversity and feasibility of CH phases under astrophysical conditions are already recognized, this study proposes an expanded range and increased feasibility of CHs in the interstellar medium.

Complex organic molecules such as methanol,[14,50,51] tetrahydrofuran,[8,12,33] and smaller ethers are known to catalyze/stabilize the formation of mixtures of nonstoichiometric CHs and this aspect has been studied experimentally as well as computationally. Therefore, small amounts of methanol formed upon photoirradiation may catalyze and stabilize the formation of CHs of CO_2 and CO. CHs of many molecules in icy planets, comets, and other extraterrestrial bodies may arise through such photochemical pathways.

Conclusions

This study suggests that the molecules formed during photochemical reactions can be trapped within CH cages even at 10 K under UHV conditions. UV photolysis is known to induce various physicochemical changes in the ice matrix, and in this study, we observed highly unusual and unique events of CH formation. These observations may likely be attributed to three factors: (1) UV light is known to heat the ice upon irradiation, (2) photochemically produced CH_3OH can act as a catalyst for CH formation, as reported in numerous studies, and (3) the photodesorption of CO, CO_2, and other species can increase the mobility of both the host and the guest molecules, which is essential for CH formation. The impact of temperature and

composition of ice mixture on such processes has been demonstrated. Trapping small molecules, radicals, and reactive species, even as they are generated through photon irradiation, holds direct significance in the context of cometary and interstellar ices. While our experiment proves the confinement of photochemical products in CH cages, the dynamics of various events leading to such cages at 10 K need additional investigations. Photochemical studies of ice mixtures can expand the diversity of CHs in interstellar environments.

Author contributions

T. P. and G. V. designed the research. G. V. and B. K. M. have performed the experiments. T. P. supervised its progress. G. V., B. K. M., R. K., and T. P. have analyzed the results. The first draft of the manuscript was written by G. V. The final version of manuscript was prepared including the contributions of all authors.

Conflicts of interest

The authors declare no competing financial interests.

Acknowledgements

We acknowledge the Science and Engineering Research Board (SERB), Department of Science and Technology (DST), Government of India for research funding. T. P. and R. K. acknowledge funding from the Centre of Excellence on Molecular Materials and Functions under the Institution of Eminence scheme of IIT Madras. G. V. thanks IITM for his research fellowships. B. K. M. thanks the Council of Scientific & Industrial Research (CSIR) for his research fellowship.

References

1 R. A. Baragiola, Water ice on outer solar system surfaces: Basic properties and radiation effects, *Planet. Space Sci.*, 2003, **51**, 953–961.
2 M. S. Westley, R. A. Baragiola, R. E. Johnson and G. A. Barattat, *Nature*, 1995, **373**, 405–407.
3 R. E. Johnson and T. I. Quickenden, Photolysis and radiolysis of water ice on outer solar system bodies, *J. Geophys. Res.: Planets*, 1997, **102**, 10985–10996.
4 E. D. Sloan Jr. and C. A. Koh, *Clathrate Hydrates of Natural Gases*, CRC Press, 2007.
5 E. D. Sloan, Fundamental principles and applications of natural gas hydrates, *Nature*, 2003, **426**, 353–359.
6 J. Ghosh, G. Vishwakarma, R. Kumar and T. Pradeep, Formation and Transformation of Clathrate Hydrates under Interstellar Conditions, *Acc. Chem. Res.*, 2023, **56**, 2241–2252.
7 J. Ghosh, R. R. J. Methikkalam, R. G. Bhuin, G. Ragupathy, N. Choudhary, R. Kumar and T. Pradeep, Clathrate hydrates in interstellar environment, *Proc. Natl. Acad. Sci. U. S. A.*, 2019, **116**, 1526–1531.
8 G. Vishwakarma, B. K. Malla, K. S. S. V. P. Reddy, J. Ghosh, S. Chowdhury, S. S. R. K. C. Yamijala, S. K. Reddy, R. Kumar and T. Pradeep, Induced Migration of CO_2 from Hydrate Cages to Amorphous Solid Water under Ultrahigh Vacuum and Cryogenic Conditions, *J. Phys. Chem. Lett.*, 2023, **14**, 2823–2829.
9 J. Ghosh, R. G. Bhuin, G. Vishwakarma and T. Pradeep, Formation of Cubic Ice via Clathrate Hydrate, Prepared in Ultrahigh Vacuum under Cryogenic Conditions, *J. Phys. Chem. Lett.*, 2020, **11**, 26–32.
10 J. Ghosh, G. Vishwakarma, S. Das and T. Pradeep, Facile Crystallization of Ice I_h *via* Formaldehyde Hydrate in Ultrahigh Vacuum under Cryogenic Conditions, *J. Phys. Chem. C*, 2021, **125**, 4532–4539.
11 B. K. Malla, G. Vishwakarma, S. Chowdhury, P. Selvarajan and T. Pradeep, Formation of Ethane Clathrate Hydrate in Ultrahigh Vacuum by Thermal Annealing, *J. Phys. Chem. C*, 2022, **126**, 17983–17989.
12 J. Ghosh, R. G. Bhuin, G. Ragupathy and T. Pradeep, Spontaneous Formation of Tetrahydrofuran Hydrate in Ultrahigh Vacuum, *J. Phys. Chem. C*, 2019, **123**, 16300–16307.
13 G. Vishwakarma, B. K. Malla, S. Chowdhury, S. P. Khandare and T. Pradeep, Existence of Acetaldehyde Clathrate Hydrate and Its Dissociation Leading to Cubic Ice under Ultrahigh Vacuum and Cryogenic Conditions, *J. Phys. Chem. Lett.*, 2023, **14**, 5328–5334.
14 D. Blake, L. Allamandola, S. Sandford, D. Hudgins, D. Blake, L. Allamandola, S. Sandford, D. Hudgins and F. Freund, Clathrate Hydrate Formation in Amorphous Cometary Ice Analogs in Vacuo, *Science*, 1991, **254**, 548–551.
15 R. P. C. Bauer, A. Ravichandran, J. S. Tse, N. Appathurai, G. King, B. Moreno, S. Desgreniers and R. Sammynaiken, In Situ X-Ray Diffraction Study on Hydrate Formation at Low Temperature in a High Vacuum, *J. Phys. Chem. C*, 2021, **125**, 26892–26900.
16 M. Choukroun, T. H. Vu and E. C. Fayolle, No compelling evidence for clathrate hydrate formation under interstellar medium conditions over laboratory time scales, *Proc. Natl. Acad. Sci. U. S. A.*, 2019, **116**, 14407–14408.
17 J. Ghosh, R. R. J. Methikkalam, R. G. Bhuin, G. Ragupathy, N. Choudhary, R. Kumar and T. Pradeep, *Proc. Natl. Acad. Sci. U. S. A.*, 2019, **116**, 14409–14410.
18 J. Shi, U. Raut, J. H. Kim, M. Loeffler and R. A. Baragiola, Ultraviolet photon-induced synthesis and trapping of H_2O_2 and O_3 in porous water ice films in the presence of ambient O_2: Implications for extraterrestrial ice, *Astrophys. J., Lett.*, 2011, **738**, L3.
19 D. A. Bahr, M. Famá, R. A. Vidal and R. A. Baragiola, Radiolysis of water ice in the outer solar system: Sputtering and trapping of radiation products, *J. Geophys. Res.*, 2001, **106**, 33285–33290.
20 F. Fleyfel and J. P. Devlin, FT-IR spectra of 90 K films of simple, mixed, and double clathrate hydrates of trimethylene oxide, methyl chloride, carbon dioxide, tetrahydrofuran, and ethylene oxide containing decoupled D_2O, *J. Phys. Chem.*, 1988, **92**, 631–635.

21 P. Goldberg, Free radicals and reactive molecules in clathrate cavities, *Science*, 1963, **142**, 378–379.
22 A. C. Cheung, D. M. Rank, C. H. Townes, D. D. Thornton and W. J. Welch, Detection of water in interstellar regions by its microwave radiation, *Nature*, 1969, **221**, 626–628.
23 R. W. Wilson, K. B. Jefferts and A. A. Penzias, Carbon Monoxide in the Orion Nebula, *Astrophys. J.*, 1970, **161**, L43.
24 S. Bag, R. G. Bhuin, R. R. J. Methikkalam, T. Pradeep, L. Kephart, J. Walker, K. Kuchta, D. Martin and J. Wei, Development of ultralow energy (1–10 eV) ion scattering spectrometry coupled with reflection absorption infrared spectroscopy and temperature programmed desorption for the investigation of molecular solids, *Rev. Sci. Instrum.*, 2014, **85**, 014103.
25 L. J. Allamandola, S. A. Sandford and G. J. Valero, Photochemical and thermal evolution of interstellar/precometary ice analogs, *Icarus*, 1988, **76**, 225–252.
26 A. Schriver, J. M. Coanga, L. Schriver-Mazzuoli and P. Ehrenfreund, FTIR studies of ultraviolet photodissociation at 10 K of dimethyl-ether in argon and nitrogen matrices, in the solid phase and in amorphous water ice, *Chem. Phys. Lett.*, 2004, **386**, 377–383.
27 G. Leto and G. A. Baratta, Ly-α photon induced amorphization of lc water ice at 16 Kelvin. Effects and quantitative comparison with ion irradiation, *Astron. Astrophys.*, 2003, **397**, 7–13.
28 N. Watanabe, O. Mouri, A. Nagaoka, T. Chigai, A. Kouchi and V. Pirronello, Laboratory Simulation of Competition between Hydrogenation and Photolysis in the Chemical Evolution of H_2O–CO Ice Mixtures, *Astrophys. J.*, 2007, **668**, 1001–1011.
29 H. Okabe, *Photochemistry of small molecules*, Wiley, New York, 1978, vol. 431.
30 H. Cottin, M. H. Moore and Y. Benilan, Photodestruction of Relevant Interstellar Molecules in Ice Mixtures, *Astrophys. J.*, 2003, **590**, 874–881.
31 P. A. Gerakines, W. A. Schutte and P. Ehrenfreund, Ultraviolet processing of interstellar ice analogs. I. Pure ices, *Astron. Astrophys.*, 1996, **312**, 289–305.
32 D. W. Davidson, Y. P. Handa, C. I. Ratcliffe, J. A. Ripmeester, J. S. Tse, J. R. Dahn, F. Lee and L. D. Calvert, Crystallographic Studies of Clathrate Hydrates. Part I, *Mol. Cryst. Liq. Cryst.*, 1986, **141**, 141–149.
33 F. Fleyfel and J. P. Devlin, Carbon dioxide clathrate hydrate epitaxial growth: spectroscopic evidence for formation of the simple type-II carbon dioxide hydrate, *J. Phys. Chem.*, 1991, **95**, 3811–3815.
34 R. Kumar, S. Lang, P. Englezos and J. Ripmeester, Application of the ATR-IR Spectroscopic Technique to the Characterization of Hydrates Formed by CO_2, CO_2/H_2 and $CO_2/H_2/C_3H_8$, *J. Phys. Chem. A*, 2009, **113**, 6308–6313.
35 R. Netsu and T. Ikeda-Fukazawa, Formation of carbon dioxide clathrate hydrate from amorphous ice with warming, *Chem. Phys. Lett.*, 2019, **716**, 22–27.
36 A. Kouchi and T. Kuroda, Amorphization of cubic ice by ultraviolet irradiation, *Nature*, 1990, **344**, 134–135.
37 B. Schmitt, J. M. Greenberg and R. J. A. Grim, The temperature dependence of the CO infrared band strength in CO:H_2O ices, *Astrophys. J.*, 1989, **340**, L33–L36.
38 E. Dartois, CO clathrate hydrate: Near to mid-IR spectroscopic signatures, *Icarus*, 2011, **212**, 950–956.
39 L. Cwiklik and J. P. Devlin, Hindering of rotational motion of guest molecules in the Type i clathrate hydrate, *Chem. Phys. Lett.*, 2010, **494**, 206–212.
40 S. Malyk, G. Kumi, H. Reisler and C. Wittig, Trapping and Release of CO_2 Guest Molecules by Amorphous Ice, *J. Phys. Chem. A*, 2007, **111**, 13365–13370.
41 A. Bar-Nun, D. Prialnik, D. Laufer and E. Kochavi, Trapping of gases by water ice and implications for icy bodies, *Icarus*, 1985, **63**, 317–332.
42 G. Notesco and A. Bar-Nun, The Effect of Methanol Clathrate-Hydrate Formation and Other Gas-Trapping Mechanisms on the Structure and Dynamics of Cometary Ices, *Icarus*, 2000, **148**, 456–463.
43 R. S. Smith, C. Huang, E. K. L. Wong and B. D. Kay, The molecular volcano: Abrupt CCl4 desorption driven by the crystallization of amorphous solid water, *Phys. Rev. Lett.*, 1997, **79**, 909–912.
44 Y. Kim, E. S. Moon, S. Shin and H. Kang, Acidic water monolayer on ruthenium(0001), *Angew. Chem., Int. Ed.*, 2012, **51**, 12806–12809.
45 M. D. Brookes and A. R. W. McKellar, Infrared spectrum of the water-carbon monoxide complex in the CO stretching region, *J. Chem. Phys.*, 1998, **109**, 5823–5829.
46 A. J. Barclay, A. Van Der Avoird, A. R. W. McKellar and N. Moazzen-Ahmadi, The water-carbon monoxide dimer: New infrared spectra,: *ab initio* rovibrational energy level calculations, and an interesting in-termolecular mode, *Phys. Chem. Chem. Phys.*, 2019, **21**, 14911–14922.
47 D. Yaron, K. I. Peterson, D. Zolandz, W. Klemperer, F. J. Lovas and R. D. Suenram, Water hydrogen bonding: The structure of the water-carbon monoxide complex, *J. Chem. Phys.*, 1990, **92**, 7095–7109.
48 Y. N. Kalugina, A. Faure, A. Van Der Avoird, K. Walker and F. Lique, Interaction of H_2O with CO: Potential energy surface, bound states and scattering calculations, *Phys. Chem. Chem. Phys.*, 2018, **20**, 5469–5477.
49 A. Ishibashi, H. Hidaka, Y. Oba, A. Kouchi and N. Watanabe, Efficient Formation Pathway of Methyl Formate: The Role of OH Radicals on Ice Dust, *Astrophys. J., Lett.*, 2021, **921**, L13.
50 K. Shin, K. A. Udachin, I. L. Moudrakovski, D. M. Leek, S. Alavi, C. I. Ratcliffe and J. A. Ripmeester, Methanol incorporation in clathrate hydrates and the implications for oil and gas pipeline flow assurance and icy planetary bodies, *Proc. Natl. Acad. Sci. U. S. A.*, 2013, **110**, 8437–8442.
51 J. P. Devlin, Catalytic activity of methanol in all-vapor subsecond clathrate-hydrate formation, *J. Chem. Phys.*, 2014, **140**, 164505–164510.

